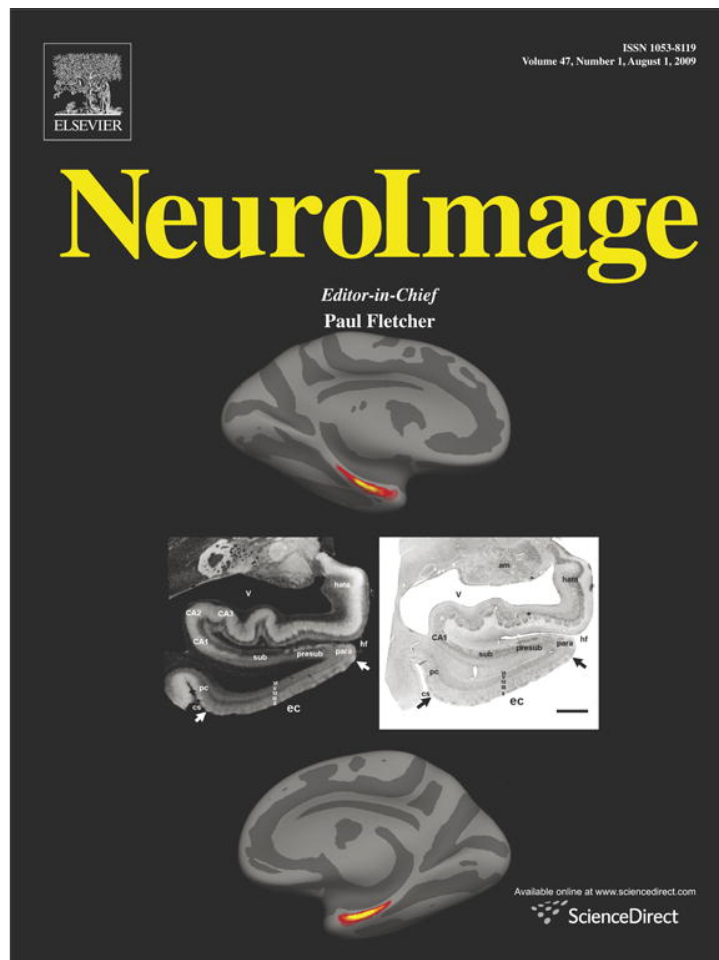


Provided for non-commercial research and education use.  
Not for reproduction, distribution or commercial use.



This article appeared in a journal published by Elsevier. The attached copy is furnished to the author for internal non-commercial research and education use, including for instruction at the authors institution and sharing with colleagues.

Other uses, including reproduction and distribution, or selling or licensing copies, or posting to personal, institutional or third party websites are prohibited.

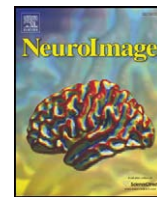
In most cases authors are permitted to post their version of the article (e.g. in Word or Tex form) to their personal website or institutional repository. Authors requiring further information regarding Elsevier's archiving and manuscript policies are encouraged to visit:

<http://www.elsevier.com/copyright>



Contents lists available at ScienceDirect

NeuroImage

journal homepage: [www.elsevier.com/locate/ynimg](http://www.elsevier.com/locate/ynimg)

## Time-variant fMRI activity in the brainstem and higher structures in response to acupuncture

Vitaly Napadow<sup>a,b,\*</sup>, Rupali Dhond<sup>a,b</sup>, Kyungmo Park<sup>c</sup>, Jieun Kim<sup>c</sup>, Nikos Makris<sup>d</sup>, Kenneth K. Kwong<sup>a</sup>, Richard E. Harris<sup>e</sup>, Patrick L. Purdon<sup>a,f,g</sup>, Norman Kettner<sup>b</sup>, Kathleen K.S. Hui<sup>a</sup>

<sup>a</sup> Athinoula A. Martinos Center for Biomedical Imaging, Department of Radiology, Massachusetts General Hospital, Charlestown, MA, USA

<sup>b</sup> Department of Radiology, Logan College of Chiropractic, Chesterfield, MO, USA

<sup>c</sup> Department of Biomedical Engineering, Kyunghee University, Yongin, Republic of Korea

<sup>d</sup> Department of Neurology, Massachusetts General Hospital, Charlestown, MA, USA

<sup>e</sup> Chronic Pain and Fatigue Research Center, Department of Anesthesiology, University of Michigan, Ann Arbor, MI, USA

<sup>f</sup> Department of Anesthesia and Critical Care, Massachusetts General Hospital, Boston, MA, USA

<sup>g</sup> Department of Brain and Cognitive Sciences, Massachusetts Institute of Technology, Cambridge, MA, USA

### ARTICLE INFO

#### Article history:

Received 22 December 2008

Revised 23 March 2009

Accepted 25 March 2009

Available online 1 April 2009

#### Keywords:

Habituation  
Cardiac gating  
Brainstem  
Alternative medicine  
Endorphin  
Dopamine  
Serotonin  
Monoamine

### ABSTRACT

Acupuncture modulation of activity in the human brainstem is not well known. This structure is plagued by physiological artifact in neuroimaging experiments. In addition, most studies have used short (<15 min) block designs, which miss delayed responses following longer duration stimulation. We used brainstem-focused cardiac-gated fMRI and evaluated time-variant brain response to longer duration (>30 min) stimulation with verum (VA, electro-stimulation at acupoint ST-36) or sham point (SPA, non-acupoint electro-stimulation) acupuncture. Our results provide evidence that acupuncture modulates brainstem nuclei important to endogenous monoaminergic and opioidergic systems. Specifically, VA modulated activity in the substantia nigra (SN), nucleus raphe magnus, locus ceruleus, nucleus cuneiformis, and periaqueductal gray (PAG). Activation in the ventrolateral PAG was greater for VA compared to SPA. Linearly decreasing time-variant activation, suggesting classical habituation, was found in response to both VA and SPA in sensorimotor (SII, posterior insula, premotor cortex) brain regions. However, VA also produced linearly time-variant activity in limbic regions (amygdala, hippocampus, and SN), which was bimodal and not likely habituation – consisting of activation in early blocks, and deactivation by the end of the run. Thus, acupuncture induces different brain response early, compared to 20–30 min after stimulation. We attribute the fMRI differences between VA and SPA to more varied and stronger psychophysical response induced by VA. Our study demonstrates that acupuncture modulation of brainstem structures can be studied non-invasively in humans, allowing for comparison to animal studies. Our protocol also demonstrates a fMRI approach to study habituation and other time-variant phenomena over longer time durations.

© 2009 Elsevier Inc. All rights reserved.

### Introduction

While many groups have investigated human brain response to acupuncture using non-invasive functional MRI (fMRI) (Dhond et al., 2007), these studies have imaged the entire brain, without any methodological modifications to focus on the brainstem – an important brain structure plagued by cardiogenic motion and susceptibility artifact in neuroimaging experiments (Dagli et al., 1999; Poncelet et al., 1992). Conversely, many studies of acupuncture mechanisms in animal models have focused on the response in brainstem structures (Cheng and Pomeranz, 1981; Han, 1998; Li et al., 2007; Tjen-A-Looi et al., 2004; Zhou et al., 2005). Thus, a careful

evaluation of human brainstem response to acupuncture is needed and may begin to bridge the gap between human and animal studies of acupuncture mechanisms. In addition, most human acupuncture fMRI studies have used a typically short (<15 min) block paradigm design. However, evidence from both clinical practice and acupuncture analgesia research studies suggests that a delayed response following longer (>20 min) acupuncture stimulation exists (Mayer, 2000). Such reports provide motivation for performing longer duration neuroimaging experiments in humans, which specifically focus on time-variant brainstem response.

Different brainstem regions have been implicated in various neurobiological models of acupuncture mechanism. For instance, endogenous opioid and monoaminergic systems are key components of brainstem processing and may be important for acupuncture mechanisms of action (Cheng and Pomeranz, 1981; Han, 2004). Evidence also exists for a delayed response (typically attributed to

\* Corresponding author. MGH/MIT/HMS Martinos Center for Biomedical Imaging, 149 13th St. Rm.2301, Charlestown, MA 02129, USA. Fax: +1 617 726 7422.  
E-mail address: [vitaly@nmr.mgh.harvard.edu](mailto:vitaly@nmr.mgh.harvard.edu) (V. Napadow).

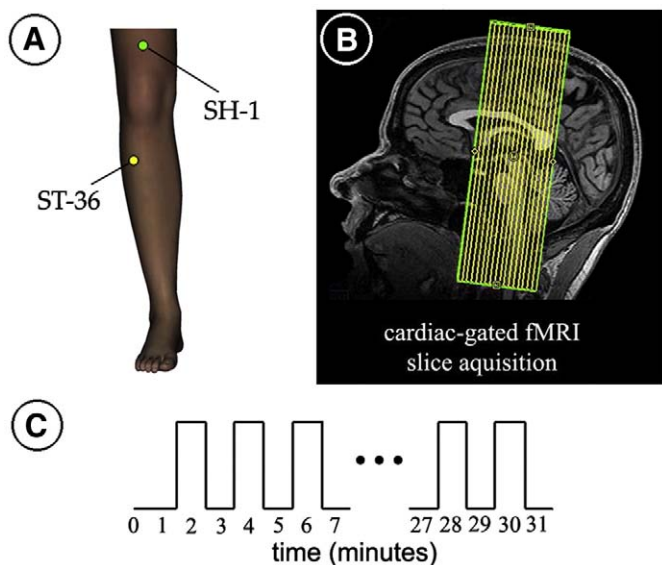


**Fig. 1.** Experimental protocol. (A) Stimulation location for both the verum acupoint (ST-36) and sham point (SH-1). (B) Cardiac-gated fMRI was performed using coronal slices covering the brainstem, as well as other cortical and subcortical structures in this field-of-view. (C) The fMRI block design paradigm consisted of alternating 1-minute stimulation and rest blocks with either electro-stimulation at acupoint ST-36 (VA) or a sham point SH-1 (SPA).

endorphinergic mechanisms), as acupuncture analgesia (AA) requires at least 20 min of continuous manual or electric needle stimulation for maximal effect (Han, 1998; Mann, 1974; Pomeranz, 2001). The monoaminergic and opioidergic systems maintain important source and target regions in the brainstem. In rats, the arcuate nucleus of the ventromedial hypothalamus contains much of the  $\beta$ -endorphin cells of the brain (Bloom and Guillemin, 1978), while the periaqueductal gray (PAG) contains large amounts of opioid receptors, enkephalin containing cell bodies and terminals, and  $\beta$ -endorphin containing terminals (Mayer, 2000). The source regions for serotonin (raphe nuclei), dopamine (substantia nigra, SN; ventral tegmental area), and noradrenaline (locus ceruleus, LC) also lie in the brainstem (Parent, 1996).

Past acupuncture fMRI studies have noted both activation and deactivation in several pontine and midbrain nuclei including the PAG (Hui et al., 2005; Liu et al., 2004; Napadow et al., 2005a,b), but no consensus has been reached. Variability in brainstem response may be due to individual variability, typically short experiment runs, or to the existence of cardiogenic pulsatile motion artifact, which serves to reduce signal-to-noise and makes anatomical localization and nuclei attribution difficult. Our approach was to mitigate the influence of cardiogenic pulsatility by gating fMRI data acquisition to the cardiac cycle (Guimaraes et al., 1998; Napadow et al., 2008; Zhang et al., 2006).

In addition, we sought to evaluate any time-variant brain response (e.g. habituation) to longer duration acupuncture stimulation. Classical habituation is the progressive decrease in physiological response to a repeating stimulus which has been deemed by the subject as neither harmful nor rewarding (Thompson and Spencer, 1966). However, other time-variant patterns of physiological response might also exist for different acupuncture-like stimuli. Hence, our experiments addressed two main questions: (1) How does the brainstem respond to acupuncture stimuli, and (2) Is there any time-variant processing of acupuncture stimuli in the brain? We hypothesized that repeated acupuncture would demonstrate habituating response in somatosensory processing regions and would also demonstrate down-regulation of limbic brain regions – an effect that would become more pronounced over time.

## Methods

This study was performed with ten (10) healthy, right-handed (Edinburgh Inventory (Oldfield, 1971)) subjects (4M, age: 21–33 years), and was approved by the Massachusetts General Hospital Subcommittee on Human Studies. Subjects were told they would receive “different forms” of acupuncture stimulation. Imaging was performed over two separate imaging sessions to accommodate the multiple, lengthy fMRI scan runs, separated by at least two days.

### Acupuncture stimulation and paradigm

Each fMRI scan run was 31.5 min in duration, during which the subject experienced one of two different stimulations: verum acupuncture (VA) or sham point acupuncture (SPA), which controlled for the location of stimulation. Each fMRI scan run began with a 90 s rest block period followed by fifteen 120 s periods of alternating stimulation (60 s) and rest (60 s) (Fig. 1C).

For VA, electro-acupuncture stimulation was used with alternating 3-second periods of 2 Hz and 15 Hz electro-stimulation (known as “dense-disperse”) at acupoint ST-36 on the lower leg (Fig. 1A). For SPA, electro-stimulation was performed with the same parameters as for VA at a sham acupoint, ~8 cm above the proximal edge of the patella, on the midline of the thigh (Fig. 1A). The reference electrode for VA was 1 cm distal to ST-36, while for SPA, it was 1 cm proximal to the sham point. Acupuncture needles were inserted before the start of each fMRI run in either the right or left leg (pseudo-randomized). Different legs were chosen for VA and SPA to avoid the possibility that long duration electro-stimulation altered segmental neural reactivity. Due to the 3 T magnetic field, we used pure-silver, non-ferrous acupuncture needles (0.25 mm diameter, 40 mm length, Maeda Corporation, Japan), inserted to a depth of approximately 2–3 cm. Electrical current was delivered with a modified current-constant H.A. N.S. (Han’s Acupoint Nerve Stimulator) LH202 (Neuroscience Research Center, Peking University, Beijing, China) for both VA and SPA. Current intensity was set by verbal subject response to be “moderately strong, but below the pain threshold” for both VA and SPA equally. Current intensity did not differ significantly (paired *t*-test,  $p > 0.1$ ) between VA ( $2.10 \pm 0.96$  mA) and SPA ( $1.94 \pm 0.89$  mA). Relatively strong stimulation and alternating frequencies were used to limit the potential for current intensity dropping below the sensory threshold over the lengthy scan run.

At the end of each fMRI scan run, subjects rated the intensity of sensations they felt during the run using a computerized i/o device. Subjects were presented with a 10 point visual analog scale (VAS) and were asked to rate the intensity of sensations commonly associated with the experience of *deqi*<sup>1</sup> and listed on the MGH Acupuncture Sensation Scale (MASS) (Kong et al., 2007a). The 10 point VAS used specific guidewords: “none” corresponding to a 0, and “unbearable” corresponding to a value of 10. Intermediate guidewords also included “mild,” which was linked to a value of 2, “moderate” which was linked to a value of 5, and “strong,” linked to a value of 8. The bar scale was presented and button box mediated responses were acquired (in increments of 0.5) with a laptop and Labview Software (Labview 7.1, DAQCard 6024E, National Instruments, Austin, Texas). A sensation was counted as present if the intensity was greater than 0.5. Subjects were also asked to assess the intensity of throbbing and sharp pain (this latter sensation is not considered to be characteristic of *deqi*). Additionally, subjects were asked to assess the extent of “spreading” that may have occurred for any of the listed sensations. A modified version of this procedure has been successfully used by our group in the past to assess psychophysical response in conjunction with

<sup>1</sup> *Deqi* corresponds to a multitude of different pain-like and non-pain sensations experienced by a needled subject (Hui et al., 2007; Kong et al., 2007a) and is a correlate of effective treatment (Vincent et al., 1989).

neuroimaging (Dhond et al., 2008; Hui et al., 2005, 2007; Napadow et al., 2005b, 2007). In order to quantify the overall, combined amplitude of *deqi* experienced, we used the *MASS-index*, which is calculated by an exponentially decreasing weighted sum of all sensations (see (Kong et al., 2007a) for details). We have developed this index as an attempt to balance the breadth and depth of sensations as well as the number of different sensations chosen by the subject. The *MASS-index* was compared between stimulation groups using a paired *t*-test, significant at  $p < 0.05$  (SPSS 10.0.7, Chicago, Illinois). Furthermore, frequency counts of specific sensations were compared between stimulation type with a Pearson Chi-squared test, significant at  $p < 0.05$ .

#### MRI data acquisition

Functional and structural scans were acquired using a 3.0 T Siemens Trio MRI System with an 8-channel head array coil equipped for echo planar imaging. Structural images were collected prior to functional imaging using a T1-weighted MPRAGE sequence (TR/TE = 2.73/3.19 ms, flip angle = 7°, FOV = 256 × 256 mm; slice thickness = 1.33 mm) in order to facilitate visualization.

BOLD functional imaging was performed using a gradient echo T2\*-weighted pulse sequence (TE = 30 ms, matrix = 64 × 64, FOV = 200 mm, flip angle = 90°) using a GRAPPA (Griswold et al., 2002) acceleration factor of 2 with our multi-channel coil. Volume acquisition was gated to the subjects' every other ECG R-wave; thus, TR varied with each acquisition (average TR was approximately 2 s). Cluster acquisition of 17 coronal slices was completed in sequential order within 926 ms. This was the maximum number of slices we could acquire (with our coil and scanner setup) within a time period which was approximately a single cardiac R–R interval. Each slice was 3 mm thick with 0.6 mm gap (voxel size 3.13 × 3.13 × 3.6 mm) and was slightly tilted to be parallel to the brainstem longitudinal axis (Fig. 1B). This orientation was chosen in order to minimize through-slice brainstem motion. Motion correction was incorporated into the fMRI scanning sequence with Prospective Acquisition Correction (PACE, Siemens Medical Systems, Erlangen, Germany) – a critical addition due to increased opportunity for head motion during our long duration scan run. More details of our cardiac-gated fMRI procedures have been previously published (Napadow et al., 2008).

Cardiac-gated acquisitions were performed to minimize physiological motion artifact due to pressure wave pulsatility in arteries within and around the brain. Our own preliminary analyses have corroborated past findings on brainstem motion and found that MRI signal fluctuation power at a typical cardiac frequency (1 Hz) was maximal in the anterior pons, medulla, tectum (e.g. inferior and superior colliculi), subgenual cingulate, and hypothalamus (Napadow et al., 2008). These regions may be plagued by diminished SNR and spurious fMRI results if cardiac pulsatility is not accounted for. As many of our autonomic structures of interest are in brain regions strongly affected by cardiogenic pulsatility, we chose to cardiac-gate our fMRI acquisition in order to reduce blurring and indeterminate voxel localization, thereby increasing fMRI sensitivity (Guimaraes et al., 1998).

#### Functional MRI analysis

Structural MRI data were co-registered to the MNI152 brain template using the Automated Brainstem Co-registration (ABC) method (Napadow et al., 2006) in order to maximize sensitivity in important brainstem and subcortical brain regions. Functional MRI data were first motion corrected with AFNI (NIH) through an iterated, linearized, weighted least-squares method with Fourier interpolation (Cox, 1996). Data runs were excluded if gross translational motion exceeded 3 mm on any axis. Any residual motion was then removed by performing probabilistic independent

component analysis (ICA) and removing components related to motion artifact (e.g. positive/negative fMRI response on opposing edges of the brain, IC timeseries spikes consistent with motion correction timeseries spikes) (Beckmann and Smith, 2004).

We performed cardiac-gated fMRI in order to reduce cardiogenic motion artifact, an approach taken by several groups at our Center (Guimaraes et al., 1998; Mainero et al., 2007; Napadow et al., 2005a, 2008; Zhang et al., 2006). However, cardiac gating produces data with variable TR, and hence variable T1-weighting. If the temporal variability of T1-weighting is significant it will overwhelm any BOLD fMRI T2\*-weighting. Thus, any MR signal fluctuation due to T1-variability must be accounted for before any model-based processing is applied. Data were corrected for T1 variability (due to variable TR) using the method detailed by Guimaraes et al. (1998). Their study clearly demonstrated improved SNR (i.e. mitigated T1-variability) in brainstem regions (the inferior colliculus for auditory stimuli) compared to non-gated fMRI. As reported by Guimaraes et al., T1 was estimated by minimizing the variance in fitting an exponential T1 decay curve to fMRI signal intensity within each voxel. The signal intensity in any given voxel can be expressed as:

$$S_{i,n} = A_{i,n} \left( 1 - e^{-\frac{t_n}{T_{1i}}} \right) \quad (1)$$

where the known variables include:  $S_{i,n}$  = signal in  $i$ th voxel,  $n$ th time point, and  $t_n$  = TR at  $n$ th time point. This expression is fit to find:  $A_{i,n}$  = max signal in  $i$ th voxel without T1 weighting, and  $T_{1i}$  = longitudinal relaxation time in  $i$ th voxel. The algorithm then uses the estimated  $A_{i,n}$  and  $T_{1i}$  to correct  $S_{i,n}$  in each voxel to the average  $t_n$  across all time points ( $T_{ave}$ ).

$$S'_{i,n} = A_{i,n} \left( 1 - e^{-\frac{T_{ave}}{T_{1i}}} \right) \quad (2)$$

This procedure uses the fMRI data itself to perform the correction, thereby avoiding spatial registration errors which would be incurred if  $T_1$  were estimated in a separate MRI scan. While the amount of correction at each time point varies with the difference between the TR and  $T_{ave}$ , and theoretically the TR could vary with variable heart rate between ON and OFF blocks, we found no difference between ON blocks and OFF blocks for both VA (ON: 63.6 ± 7.8 bpm, OFF: 64.0 ± 7.9, paired *t*-test:  $p = 0.20$ ) and SPA (ON: 64.2 ± 10.6, OFF: 64.2 ± 10.9, paired *t*-test:  $p = 0.92$ ). Thus, the difference in mean R–R between ON and OFF blocks for VA was on the order of 5.9 ms.

In addition, error in the estimated  $T_1$  may have been propagated to an error in BOLD signal correction. In order to estimate this propagated error we calculated the variability in  $T_1$  (standard deviation of  $T_1$ , or  $\sigma(T_1)$ ) within several significant brainstem clusters. Using our collected data we assume an average TR to which all time points are corrected to be  $T_{ave} = 1900$  ms. Also using our data, we take the average correction time to be  $\Delta t = 81.5$  ms. Then, using our calculated mean  $T_1$  for each region, and assuming a  $T_1' = T_1 + \sigma(T_1)$ , as calculated for each region, we can compute the propagated percent error in the correction of signal intensity (%CorErr) as:

$$\%CorErr = \frac{\left[ \left( 1 - e^{-\frac{T_{ave}}{T_1}} \right) - \left( 1 - e^{-\frac{T_{ave} + \Delta t}{T_1}} \right) \right] - \left[ \left( 1 - e^{-\frac{T_{ave}}{T_1'}} \right) - \left( 1 - e^{-\frac{T_{ave} + \Delta t}{T_1'}} \right) \right]}{\left[ \left( 1 - e^{-\frac{T_{ave}}{T_1}} \right) - \left( 1 - e^{-\frac{T_{ave} + \Delta t}{T_1}} \right) \right]} \times 100 \quad (3)$$

This error represents the effect of using  $T_1'$  instead of  $T_1$  in correcting a TR at  $T_{ave} + \Delta t$  to  $T_{ave}$ .

We found the following mean  $T_1$ , standard deviations, and propagated correction error for each of 3 representative ROIs: locus ceruleus ( $T_1$ : 1152.6 ms,  $\sigma(T_1)$ : 226.3 ms, %CorErr: 8.92%), PAG ( $T_1$ : 1261.9 ms,  $\sigma(T_1)$ : 131.1 ms, %CorErr: 4.06%), substantia nigra ( $T_1$ : 1108.1 ms,  $\sigma(T_1)$ : 101.5 ms, %CorErr: 5.45%). Thus, the propagated

**Table 1**  
Brainstem nuclei modulated by acupuncture (VA and SPA).

	Side	Location (axial coordinate, z)	VA Z-score	SPA Z-score	VA – SPA Z-score
<i>Verum acupuncture (ST-36)</i>					
Nucl raphe pal/nucl raphe magnus	n/a	Obex + 10	−4.31	n/a	n/a
NTS/vestib nucl cmplx	R	Obex + 12	−4.41	n/a	n/a
Parabrachial nucleus	R	Obex + 22	−4.54	n/a	n/a
Locus ceruleus	R	Obex + 22	−3.04	n/a	n/a
	L	Obex + 24	−3.90	n/a	n/a
Reticulo-tegmental/pontine nuclei	L	Obex + 27	−4.10	n/a	n/a
Nucleus cuneiformis	R	Obex + 34	−4.50	n/a	n/a
PAG	L	Obex + 42	−4.00	n/a	n/a
	L	Obex + 50	3.99	n/a	n/a
Inferior colliculus	L	Obex + 46	−4.09	n/a	n/a
Substantia nigra	R	Obex + 48	2.70	n/a	n/a
Superior colliculus	R	Obex + 54	4.26	n/a	n/a
<i>Sham point acupuncture (SH-1)</i>					
None					
<i>Verum &gt; sham point acupuncture</i>					
Substantia nigra	L	Obex + 48	3.76	−0.62	3.10
Red nucleus	R	Obex + 48	1.36	−3.75	3.63
PAG	L	Obex + 50	4.25	−2.59	4.80
Superior colliculus	R	Obex + 54	4.78	−2.32	4.99
<i>Sham point &gt; verum acupuncture</i>					
Inferior colliculus	L	Obex + 46	−4.68	0.22	−3.58

Results for both main effect and the VA – SPA contrast are listed. Location is referenced relative to the obex in the medulla (roughly at  $z = -57$  mm in MNI-space, see Fig. 2). Z-stat is listed for most activated/deactivated voxel.

error to the correction of a typical time point in these brainstem regions is roughly only 4–8% of the original correction. Our actual T1 correction for the ROI's above (comparing corrected with uncorrected BOLD data) corresponded to an average percent signal change of 2% or less: locus ceruleus ( $1.8 \pm 0.2\%$ ,  $\mu \pm \sigma$ ), PAG ( $2.0 \pm 0.3\%$ ), substantia nigra ( $1.6 \pm 0.3\%$ ). Thus we do not expect that a 4–8% error in this correction (resulting in a % signal change error of 0.08–0.16%), arising from a roughly 10–20% error in T1, would have a large impact on percent signal change calculations in our regions of interest.

It should also be noted that other viable options for physiological noise correction exist, and include cardiac gating with T1-correction using a T1-map calculated in scans different from the original BOLD data (Malinen et al., 2006), as well as non cardiac-gated retrospective algorithms using concurrently collected ECG data (Glover et al., 2000).

Only minimal spatial smoothing, on the order of a voxel, (FWHM = 3 mm) was performed on the fMRI data, as some brainstem nuclei are on the order of image voxel size. The data were also high-pass filtered in the temporal domain ( $f_{\text{high}} = 0.0083$  Hz) to remove baseline signal drifts. Corfield et al. found that high-pass filtering with this cutoff frequency yielded similar results to more intensive artifact mitigation procedures such as regressing out cardiac and respiratory phase timings in a general linear model (Corfield et al., 1999).

Statistical parametric mapping at the single-subject level was completed via a generalized linear model (GLM) by using FMRI Expert Analysis Tool (FEAT, FSL). Time-series statistical analysis was carried out using FILM (FMRIB's Improved Linear Model) with local autocorrelation correction. The hemodynamic response function utilized in the GLM analysis was defined by the block design paradigm convolved with a prescribed gamma function (standard deviation = 3 s, mean lag = 6 s). The block paradigm was defined to be "1" during the 1-minute ON blocks and "0" during the 1-minute OFF blocks. As we wanted our analysis to be sensitive to time-variant signal increase and signal decrease response patterns, we did not use a single ON–OFF block design that encompassed the full run duration. Instead, each of the 15 ON blocks was modeled with a separate block step function regressor convolved with a canonical gamma HRF model. This approach allowed for analysis of the time varying response of the BOLD signal for each voxel, something not typically

done in traditional fMRI block design analysis which has fewer blocks and much shorter scan run durations.

Main effect and time-variant group response was calculated at the second level by passing up each subject's parameter estimate (and its variance) for each of the 15 regressors defined above. For the brainstem specific analysis, ABC-adjusted standard space parameter estimates (and their variance) from individual subjects were imported to a group level analysis with FLAME (FMRIB's Local Analysis of Mixed Effects, using a Markov Chain Monte Carlo (MCMC)-based mixed-effects analysis). The same was done in MNI-space to infer activation/deactivation in cortical and subcortical structures rostral to the brainstem. As stimulation site was pseudo-randomized to be right or left, we performed two MNI-space analyses, one which flipped left-sided stimulation data across the mid-sagittal plane in order to infer activity in brain structures likely to respond contralateral to the stimulus side (thalamus, SI and SII, posterolateral parietal), and one which kept the data in its original right-left configuration (all other structures). For both VA and SPA, contrast parameters at the group level were specified which derived (1) the "main effect" across all 15 blocks from all subjects and (2) linear time-variant (decrease or increase) response. The latter was calculated by creating a contrast where the group response for each of the 15 blocks was weighted by a linearly decreasing factor, from 7 to −7 (zero mean). We chose not to set a single EV with linear scaled block-weighting at the first level because we wanted our analysis to differentiate between significant linear decreases manifest as strong activation in the beginning of the run trailing off to no activation at the end, versus a significant linear decrease where there is no activation in the beginning of the run but strong deactivation at the end. By estimating time-variant response as a group level contrast (collapsed over all subjects in the analysis for each block), and by plotting the time-variant GLM coefficients, the above two scenarios can be differentiated.

Both VA and SPA parameter estimates were also placed in a mixed-effects group level analysis in order to directly compare the two forms of stimulation with a VA – SPA contrast. For brainstem data, where activation clusters were expected to be small, resultant statistical parametric maps for the main effect and linear time-variant effect were cluster corrected (Gaussian Random Field theory) for multiple comparisons at  $p < 0.01$ . For cortical and subcortical (but supra-

brainstem) data, the main effect and linear time-variant group maps were threshold at a cluster corrected  $p < 0.001$ . Average time courses (Fig. 5) from distinct brain regions were created by first resampling single-subject fMRI data to an average TR of 2 s.

Classical habituation was defined in our linearly time-variant results by using the following criteria: (1) robust activation (positive

percent signal change greater than 1 standard deviation from nil) for the first 3 blocks, (2) linear decrease in time, and (3) minimal response (percent signal change within 1 standard deviation of nil) for the last 3 blocks (see Table 2).

In order to test if the results of our psychophysical analysis correlated with inter-subject variability in fMRI response to the

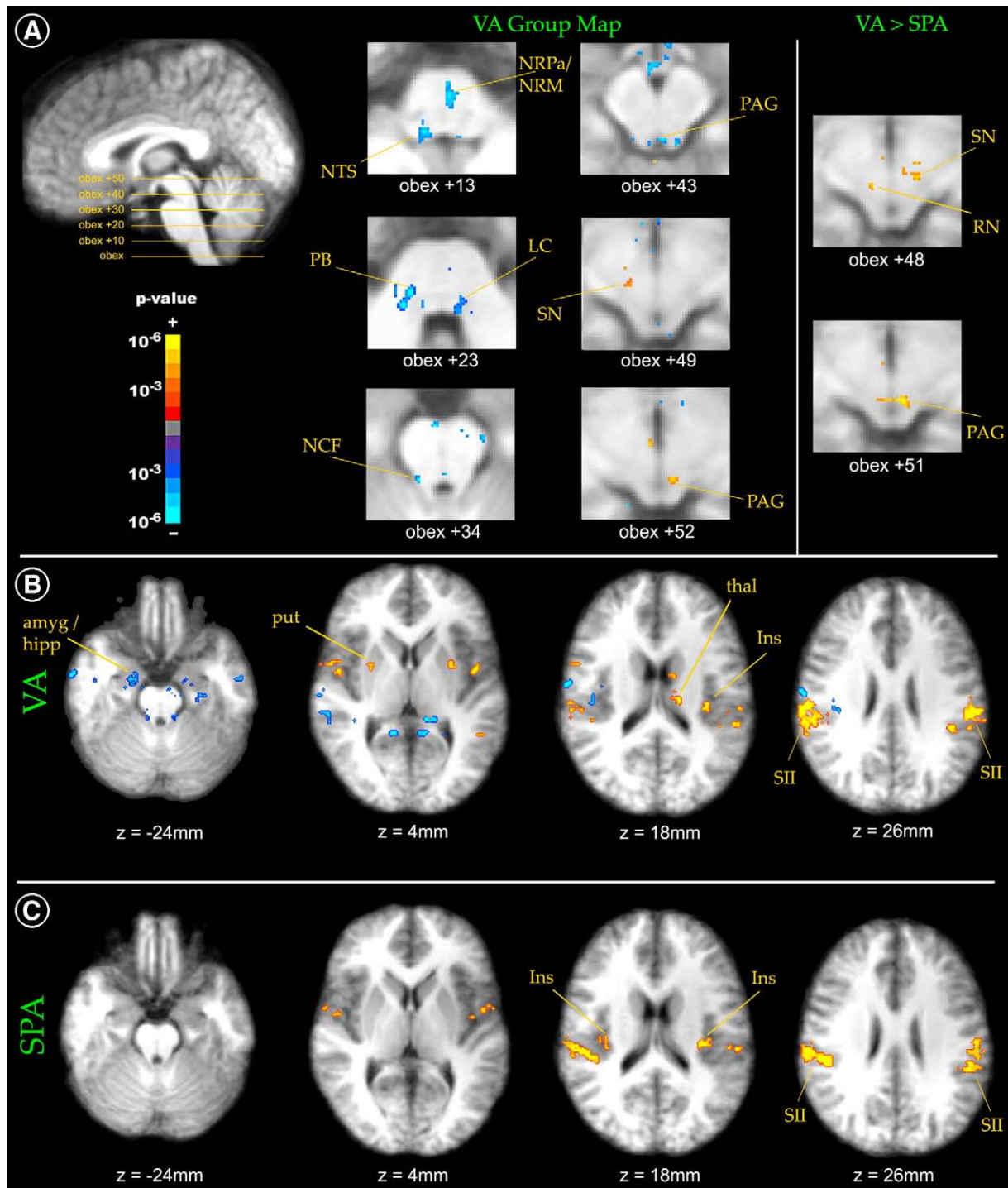


**Fig. 2.** (A) Group maps of the main effect for brainstem activation/deactivation elicited by verum (VA) and sham point (SPA) acupuncture. While VA induced both activation and deactivation in several brainstem nuclei, brainstem fMRI response at the same threshold was not found for SPA. A direct comparison of VA and SPA found that VA induced greater activation in the rostral ventrolateral PAG, SN, and RN. Axial slices are presented relative to the obex, a medullary landmark. The group maps for main effect in supra-brainstem regions is also presented for both (B) VA and (C) SPA. LC = locus ceruleus, NCF = nucleus cuneiformis, NRM = nucleus raphe magnus, NRPa = nucleus raphe pallidus, NTS = nucleus tractus solitarius, PAG = periaqueductal gray, PB = parabrachial nucleus, RN = red nucleus, SN = substantia nigra, amyg = amygdala, hipp = hippocampus, put = putamen, thal = thalamus, Ins = insula.

stimuli, we performed a mixed-effects ANCOVA, with the de-measured MASS-index from each subject as the covariate of interest. This analysis was performed separately for both VA and SPA, using group analysis methods identical to those above. For the MNI-analyses, data were corrected for multiple comparisons at a cluster corrected  $p < 0.05$  (reflecting the relatively lower degrees of freedom in this ANCOVA).

#### Anatomical localization

Anatomical localization for forebrain neuroimaging data was aided by a stereotaxic (Talairach coordinate system) atlas (Mai et al., 2004). Given that the Talairach or MNI coordinate system is not specific for the brainstem, we adopted a previously validated approach (DaSilva et al., 2002) under supervision of one of the investigators (NM), who is an experienced neuroanatomist. Briefly, localization was performed using a landmark-based topographical methodology wherein the human brainstem has been subdivided into 28 distinct regions of interest or parcellation units (PUs). These PUs included the rostral dorsal medulla (site of DMNX, NTS, and NAmb) and rostral dorsal pons (site of PBN, and locus ceruleus, LC), which were of principal interest in the present study. Activity within the PUs was assessed for consistency with known brainstem nuclei using an atlas (Paxinos and Huang, 1995). In lieu of an MNI coordinate, we reference the location of brainstem activation clusters in an axial plane relative to a medullary landmark – the obex (located roughly at MNI  $z = -57$  mm on our group averaged anatomical volume, see Figs. 2 and 3). Furthermore, based on our estimates from postmortem human material and those reconstructed from anatomical atlases (Paxinos and Huang, 1995), we can calculate the values for three representative structures – one small (locus ceruleus: approximately  $27 \text{ mm}^3$ ), one medium-sized (inferior colliculus: approximately  $180 \text{ mm}^3$ ), and one large (substantia nigra: approximately  $570 \text{ mm}^3$ ). The rest of the structures are in-between these estimates. Given our voxel size, partial-volume effects would certainly be present for the smaller brainstem nuclei, and so we have used the phrase “consistent with” when attributing results to specific brainstem nuclei, reflecting this uncertainty.

## Results

All subjects were able to complete the stimulation fMRI scan runs without excessive motion artifact and without falling asleep (by self report). One subject was not able to return for their SPA scan.

#### fMRI results: main effect

Group maps summarizing the main effect for all 15 stimulation blocks demonstrated differences in brainstem response between VA and SPA (Table 1, Fig. 2). As many of these brainstem nuclei are small (on the order of a one or two voxels in their smallest dimension), in order to be as conservative as possible, our designations are split into two adjacent nuclei where appropriate. VA was found to induce activation in regions consistent with the ventrolateral PAG, SN, and superior colliculus. Deactivation was found in regions consistent with the nucleus raphe pallidus/nucleus raphe magnus (NRM), nucleus tractus solitarius/vestibular nuclear complex, parabrachial nucleus (PBN), locus ceruleus, reticulo-tegmental/pontine nuclei, nucleus cuneiformis (NCF), inferior colliculus, and caudal ventrolateral and lateral periaqueductal gray (PAG). In contrast, SPA did not induce any significant activations or deactivations in the brainstem at our threshold. Furthermore, the contrast VA>SPA found a significant difference (due to VA activation and a trend for SPA deactivation) in regions consistent with the rostral ventrolateral PAG, SN, and right superior colliculus. Conversely, VA>SPA significance in the red nucleus (RN) was mainly driven by deactivation for SPA. In addition,

SPA>VA significance in the inferior colliculus was mainly driven by deactivation for VA.

While not the focus of our study, main effect results in supra-brainstem regions were generally consistent with our past whole-brain, non cardiac-gated experiments (Hui et al., 2000; Hui et al., 2005; Napadow et al., 2005b, 2007). For VA, this response included activation in secondary somatosensory cortex (SII), thalamus, insula, putamen, posterolateral parietal cortex, premotor cortex (PMC) and supplementary motor area (SMA)) and higher cortical (prefrontal cortex) areas (Fig. 2). SPA-induced activation was less widespread, but did include bilateral insula and SII. There was also deactivation in limbic (amygdala and hippocampus) and prefrontal cortical areas, which was more robust for VA compared to SPA.

#### fMRI results: linear time-variant response

The results of our time-variant analysis yielded interesting similarities and differences between VA and SPA (Table 2). For instance, both modes of stimulation produced activation, which decreased linearly in time, within sensorimotor brain regions such as bilateral insular cortex, PMC, and SII (Figs. 3 and 4). However, VA also induced linearly decreasing response in the posterior Middle Cingulate Cortex (pMCC, consistent with BA 24), supra-marginal gyrus (SMG), and the posterior superior temporal gyrus (STG). In addition, VA induced linearly decreasing response in other sensorimotor regions such as the SMA and dorsal posterior cingulate cortex (dPCC, consistent with BA 23). Interestingly, VA also produced linear decrease in higher cognitive regions (dorso-lateral prefrontal cortex, DLPFC, consistent with BA 8) and several limbic regions where the response to early blocks was activation, which switched to deactivation by the latter blocks in the run (Fig. 3). These limbic regions included the amygdala, hippocampus, and several brainstem regions consistent with the SN and PBN. Other brainstem nuclei that exhibited linearly decreasing response included the ventral tegmental area (VTA), ventrolateral PAG, and superior colliculus. While our contrast tested for linear effects, some non-linear patterns were also seen. There was a fundamentally different fMRI response to VA in the SN during the first 6 blocks (activation), compared to the last 3 blocks (deactivation), which did not subjectively appear linear (when plotting out parameter estimates), though it was captured by the linear regressor (Fig. 5). Also, it should be noted that the linearly decreasing cluster in the amygdala was specific to the centromedial nucleus and was spatially distinct from another amygdala cluster in the basolateral nucleus, which demonstrated deactivation on the group map for the mean response over the entire run (Supplementary Fig. 1).

#### Results of psychophysical analysis

A significant main effect due to stimulation type was found for MASS-index, a summary measure of *deqi* intensity (Fig. 6). The MASS-index was greater for VA ( $5.6 \pm 1.8$ ,  $\mu \pm \sigma$ ) compared to SPA ( $4.4 \pm 2.7$ ), by paired *t*-test ( $p < 0.05$ ).

Differences also existed between VA and SPA in regard to the types of *deqi* sensations elicited (Fig. 6). Specifically, the prevalence of aching (VA: 100% of subjects, SPA: 44.4%,  $p < 0.001$ ), was greater for VA compared to SPA. Sharp pain was reported in about half of runs for both stimulation types, though it should be noted that when debriefed, most subjects who reported sharp pain described this sensation as only transient, occurring typically at the start of a stimulation block. Pure silver needles were used for safety reasons, as they are non-magnetic. However, silver is soft and needles made from this metal are difficult to manufacture without leaving burrs and imperfections. These needle imperfections may have contributed to a higher propensity for sharp pain than what would be expected for

**Table 2**  
Linear time-variant response to acupuncture (VA and SPA).

	Side	Location (MNI)			Z-score	1st 3 Blocks	Last 3 Blocks
		X	Y	Z			
<i>Verum acupuncture (ST-36)</i>							
Parabrachial nucleus	L	Obex + 32			3.70	0.26 ± 0.12	− 0.15 ± 0.10
Substantia nigra	R	Obex + 43			4.34	0.30 ± 0.11	− 0.19 ± 0.07
Ventral tegmental area	n/a	Obex + 50			3.54	0.19 ± 0.12	− 0.10 ± 0.11
Periaqueductal gray	L	Obex + 50			3.56	0.25 ± 0.10	− 0.08 ± 0.11
Superior colliculus	L	Obex + 53			3.70	0.32 ± 0.15	− 0.16 ± 0.17
Amygdala	R	21	− 4	− 15	4.23	0.37 ± 0.20	− 0.21 ± 0.11
Hippocampus	R	26	− 21	− 10	4.27	0.30 ± 0.15	− 0.28 ± 0.18
Dorsolateral prefrontal cortex (ba8)	L	− 23	6	69	5.00	0.29 ± 0.23	− 0.46 ± 0.20
Premotor cortex	R	48	2	40	5.56	0.61 ± 0.27	− 0.06 ± 0.14
	L	− 47	4	39	5.40	0.44 ± 0.26	− 0.17 ± 0.15
Insula	R	39	− 4	− 13	5.02	0.29 ± 0.14	− 0.11 ± 0.12
	L	− 37	− 11	6	5.49	0.37 ± 0.20	− 0.11 ± 0.13
Posterior middle cingulate cortex	R	3	− 15	46	5.78	0.35 ± 0.16	− 0.23 ± 0.17
Posterior cingulate cortex	R	1	− 38	24	4.31	0.37 ± 0.18	− 0.28 ± 0.14
SII	R	62	− 16	13	4.34	0.64 ± 0.27	− 0.18 ± 0.22
	L	− 52	− 16	14	4.32	0.68 ± 0.09	0.02 ± 0.12
Supramarginal gyrus	R	52	− 24	42	4.10	0.40 ± 0.24	− 0.19 ± 0.21
	L	− 52	− 25	40	4.70	0.43 ± 0.18	− 0.12 ± 0.19
Superior temporal gyrus	R	58	− 43	16	4.51	0.26 ± 0.15	− 0.31 ± 0.16
	L	− 59	− 41	16	4.36	0.35 ± 0.17	− 0.20 ± 0.15
Supplementary motor area	R	4	− 15	75	5.08	0.78 ± 0.27	− 0.20 ± 0.26
<i>Sham point acupuncture (SH-1)</i>							
Premotor cortex	L	− 46	− 4	33	4.23	0.31 ± 0.16	− 0.08 ± 0.12
Insula	R	44	− 8	− 3	4.73	0.32 ± 0.14	− 0.12 ± 0.13
	L	− 36	− 13	− 4	4.82	0.22 ± 0.13	− 0.13 ± 0.12
SII	R	56	− 26	17	4.66	0.48 ± 0.16	− 0.04 ± 0.15
	L	− 52	− 22	23	4.68	0.47 ± 0.11	0.04 ± 0.11

All listed structures demonstrated linearly decreasing (and not increasing) response. The percent signal change mean and standard deviation for the first 3 blocks and the last 3 blocks in the scan run is listed in the two rightmost columns. These data are shaded if they are consistent with classical habituation (see [Methods](#) for criteria).

acupuncture with typical silicon-coated (or even uncoated) stainless steel needles.

We also performed an ANCOVA with the results of our MASS-index metric in order to test if subjects' brain response to VA and SPA stimulation covaried with acupuncture sensation experienced by these same subjects. While there were no significant results for SPA, the ANCOVA results for VA found that fMRI response in the right posterior Middle Cingulate Cortex (pMCC:  $x/y/z = 6/6/38$ ,  $z = 3.12$ ,  $r = 0.89$ ) and right middle temporal gyrus (MTG:  $x/y/z = 48/-28/1$ ,  $z = 3.43$ ,  $r = 0.92$ ) covaried positively with MASS-index ([Fig. 7](#)). In other words, greater sensation intensity yielded greater brain response in these areas, suggesting that the pMCC and MTG are at least partially responsible for coding sensation intensity to VA stimulation.

## Discussion

Our results provide evidence that acupuncture modulates brainstem nuclei important to endogenous monoaminergic and opioidergic systems. Specifically, VA produced activation in the SN, a source of dopaminergic tone, and deactivation in the NRM (serotonergic), locus ceruleus (noradrenergic), and the PAG (opioidergic and monoaminergic). Activation in the ventrolateral PAG was greater for VA compared to SPA. Linearly decreasing time-variant activation, suggesting classical habituation, was found in response to both VA and SPA in sensorimotor (SII, posterior insula, and PMC) brain regions. However, only VA produced linearly time-variant fMRI activity in limbic regions, such as the amygdala, hippocampus, and SN. Moreover, this response was bimodal and not likely habituation, as initial activation transitioned to a delayed deactivation by the last 3 blocks in the run. These data show that acupuncture induces different brain response early in the course of stimulation, compared to 20–30 min after stimulation has commenced. Furthermore, our study demonstrates that acupuncture modulation of brainstem structures can be

studied non-invasively in humans, allowing for comparison to the more typical invasive studies in anesthetized animal models.

### Time-variant response to acupuncture in the somatosensory system

We noted activation, which was linearly decreasing in time, within several structures important to sensorimotor processing for both VA and SPA. These structures included bilateral insular cortex, PMC, and SII. The insular habituation was toward the posterior portion of this structure, an area purported to process sensory/discriminative, rather than affective information ([Craig et al., 2000](#)). As both VA and SPA conferred a somatosensory stimulus to the body, this habituation should not be surprising. VA also produced habituating activation in other sensorimotor structures such as the SMG, STG, and SMA. The posterior STG is a multimodal sensory area, receives input from the posterior insula ([Hackett et al., 2007](#)) and is commonly activated in somatosensory studies. Furthermore, the pMCC showed linearly decreasing time-variant response to VA and appeared important in coding acupuncture sensation intensity. This region (and the dorsal PCC which responded to VA) is functionally distinct from the limbic/affective anterior cingulate cortex (ACC, which was outside our field-of-view), and interacts with the posterolateral parietal cortex in orienting the body in response to somatosensory stimuli ([Vogt, 2005](#)) — a function also ascribed to the superior colliculus ([Meredith and Stein, 1986](#); [Nagy et al., 2006](#)), which was found to be activated to a greater extent for VA compared to SPA ([Fig. 2](#)).

### Time-variant response to acupuncture in higher cognitive structures

The DLPFC demonstrated linearly decreasing bimodal time-variant activation for VA. This response was seen in a subregion consistent with the caudal dorsolateral prefrontal region (BA 8), which is interconnected with superior temporal (e.g. STG) and inferior parietal areas (e.g. SMG) — two regions which demonstrated habituation for

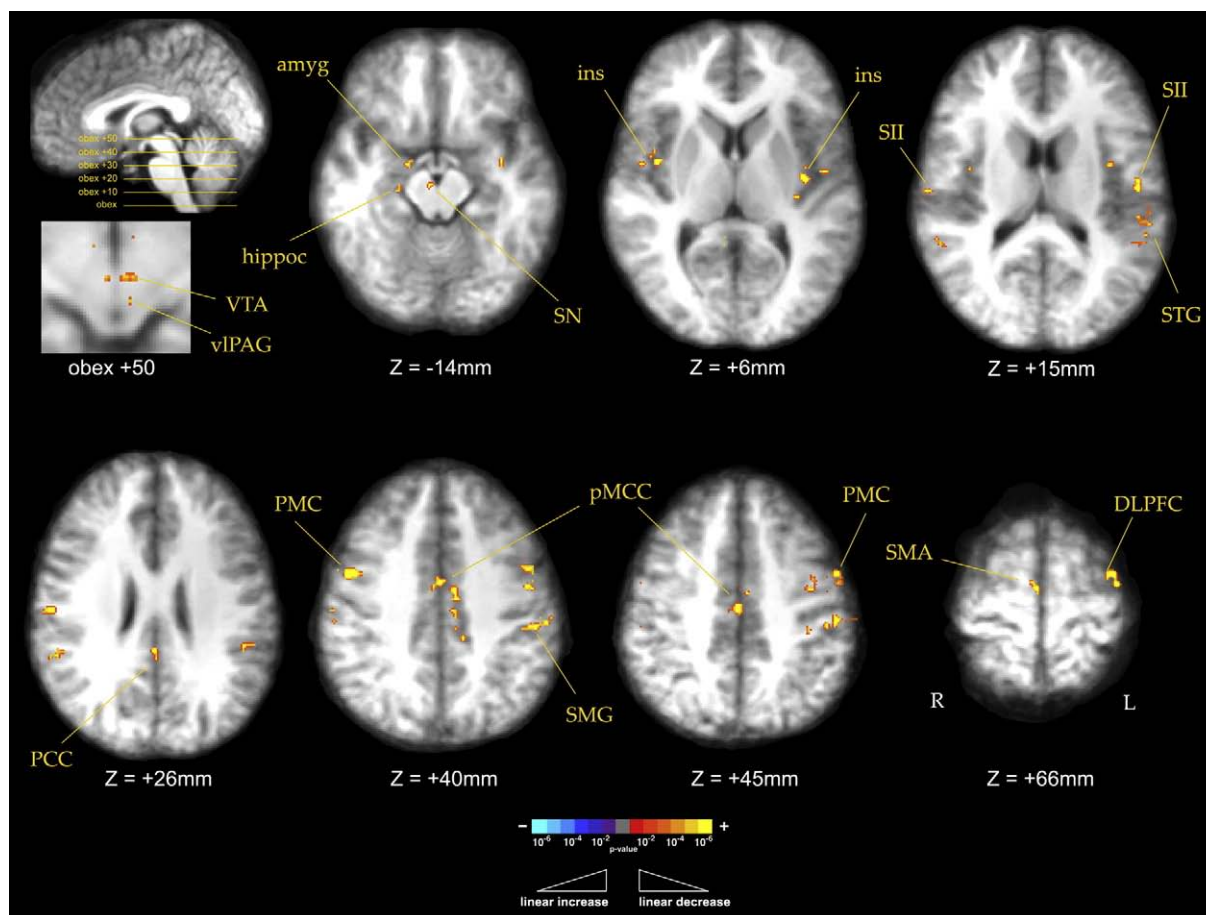


**Fig. 3.** Group map of linear time-variant response for verum acupuncture (VA) in brainstem, cortical, and subcortical brain structures. Red/yellow clusters represent fMRI response which linearly decreases from block to block, while blue/cyan clusters (none found) represent linearly increasing response. vIPAG = ventrolateral periaqueductal gray, VTA = ventral tegmental area, SN = substantia nigra, hippoc = hippocampal formation, amyg = amygdala, ins = insula, SII = secondary somatosensory cortex, STG = posterior superior temporal gyrus, PCC = dorsal posterior cingulate cortex, PMC = premotor cortex, SMG = supramarginal gyrus, pMCC = posterior middle cingulate cortex, DLPFC = dorsolateral prefrontal cortex, SMA = supplementary motor area.

VA. This DLPFC subregion has been linked with attention allocation to competing stimuli (Petrides, 2005). VA was found to induce a more diverse and stronger psychophysical experience (Fig. 6). Perhaps VA was more apt to recruit attention networks when somatosensory processing was greater (and the stimulus more novel) in the beginning compared to the end of the scan run – leading to this time-variant fMRI response. Unfortunately our field-of-view precluded time-variant assessment of more rostral, executive DLPFC regions.

#### Time-variant response to acupuncture in the limbic system

Several limbic structures also responded to VA with linearly time-variant activity. However, this pattern was best characterized by early activation giving way to later (delayed) deactivation (Fig. 5), as opposed to the simply decreasing activation (habituation) seen in somatosensory structures. One of these limbic regions was the amygdala, a key region for processing emotion (particularly fear) and motivation (Sah et al., 2003; Zald, 2003). Amygdala deactivation has been reported for acupuncture (Hui et al., 2000, 2005; Napadow et al., 2005b, 2007) and even pain (Becerra et al., 1999, 2001; Derbyshire et al., 1997; Petrovic et al., 1999, 2004) stimuli. This amygdalar deactivation may serve as a cognitive coping mechanism for pain suppression (Hsieh et al., 1999; Petrovic and Ingvar, 2002), and, as it was found to be more pronounced in chronic pain patients in response to acupuncture (Napadow et al., 2007), could be related to a therapeutic mechanism for acupuncture in chronic pain. In fact, the

delayed deactivation in the amygdala may be related to the delayed analgesia noted for acupuncture (Han, 1998; Mann, 1974; Pomeranz, 2001). Interestingly, while “main effect” deactivation was found in the basolateral nucleus of the amygdala, the centromedial amygdalar nucleus demonstrated linearly time-variant response to VA – activation early and deactivation late (Supplementary Fig. 1). Although both nuclei regulate affect and motivation, the basolateral nucleus has been implicated in assigning affective states to sensory stimuli, while the centromedial nucleus translates these affective states to autonomic signatures via projections to the hypothalamus and brainstem, thereby influencing behavioral response (Sah et al., 2003).

The hippocampus also demonstrated linearly time-variant activity to VA. This limbic structure is crucial for memory consolidation and, as a component of the default-mode network (Raichle et al., 2001), is deactivated by acupuncture (Hui et al., 2000, 2005; Napadow et al., 2005b) as well as other externally directed stimuli (Buckner et al., 2008). The time-variant response found in this study suggests that activity in this area changes over time during acupuncture stimulation and is consistent with our previous finding that connectivity between this area and the default-mode network is enhanced not just during acupuncture stimulation, but also in a resting state after stimulation has ceased (Dhond et al., 2008)

Acupuncture response in limbic brainstem regions (VTA, PAG, SN) will be discussed below. Time-variant response in these limbic structures was not seen for SPA.

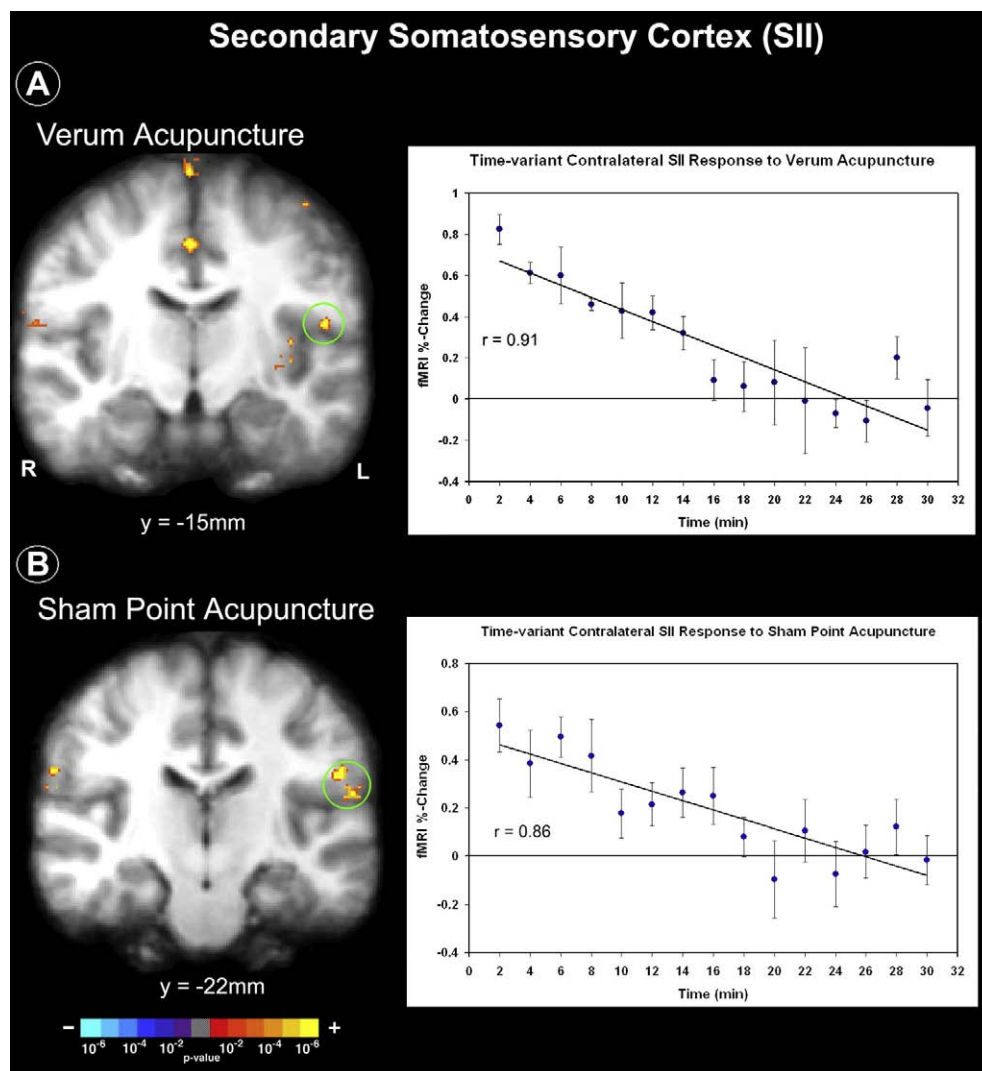


**Fig. 4.** Classical habituation in SII. Linearly time-variant signal decrease across blocks was found for both [A] verum acupuncture (VA), and [B] sham point acupuncture (SPA). By the end of the run, portions of SII (as well as other somatosensory structures) had negligible block response to stimulation.

#### Acupuncture modulation of monoaminergic and opioidergic brainstem networks

Synthesis of data across animal and human studies suggests that multiple neurotransmitters are involved in the generation of acupuncture effects. Although endogenous opioid peptides have been widely reported to play a major role in acupuncture analgesia (Han, 2004; Mayer, 2000; Pomeranz and Chiu, 1976), they cannot explain all of the physiological effects of acupuncture on the cardiovascular, respiratory, gastrointestinal, endocrine, and even pain systems. Diffusely projecting monoaminergic systems (dopamine, serotonin, noradrenaline) also modulate brain structures in limbic and higher cortical networks, and likely play an important role in addition to the endogenous opioidergic system (Mayer, 2000). While our fMRI approach does not sample neurotransmitter levels, our data infers brain activity for known source or target regions from monoaminergic and opioidergic networks. Thus, to place our brainstem results into proper context, a discussion vis-à-vis the existing animal literature is warranted.

Studies in animal models have shown that acupuncture modulates DA neurotransmission. For example, DA down-regulation has been noted in several animal models (Han et al., 1999; Wang et al., 1999). Our results in the human clearly show that VA modulates activity in the VTA and SN, a source of dopaminergic tone to higher brain

structures (Figs. 2 and 3). VA induced activation in the SN, and a slightly different SN region was found to have activation to early VA stimuli, and deactivation to late (>25 min) stimuli (Fig. 5). In comparison, acupuncture-induced SN deactivation in previous studies (Hui et al., 2005) may have been due to differences in brain response to electrical versus manual needle stimulation. However, we did find SN deactivation in latter blocks, which is also consistent with DA down-regulation in animal models following longer duration (40 min) EA at the same acupoint on the leg, ST-36 (Wang et al., 1999). In general, difficulties in comparing our human neuroimaging results with those using invasive methods in animal models remain. While similarities exist, differences could be easily attributed to species differences and awake versus anesthetized states; both of which lead to variable influences of cognitive, top-down modulation on lower brainstem regions.

Acupuncture modulation of serotonin (5-HT) has also been investigated with animal models and this system is important for both disorders of pain and affect. Electroacupuncture appears to increase 5-HT synthesis and utilization in the rat (Han et al., 1979), specifically in the DRN and NRM (Kwon et al., 2000). Our results in the human demonstrated NRM deactivation for VA.

Noradrenaline (NA) modulation by acupuncture was supported by LC deactivation in response to VA. The LC is the source of noradrenergic input to higher forebrain structures and is associated

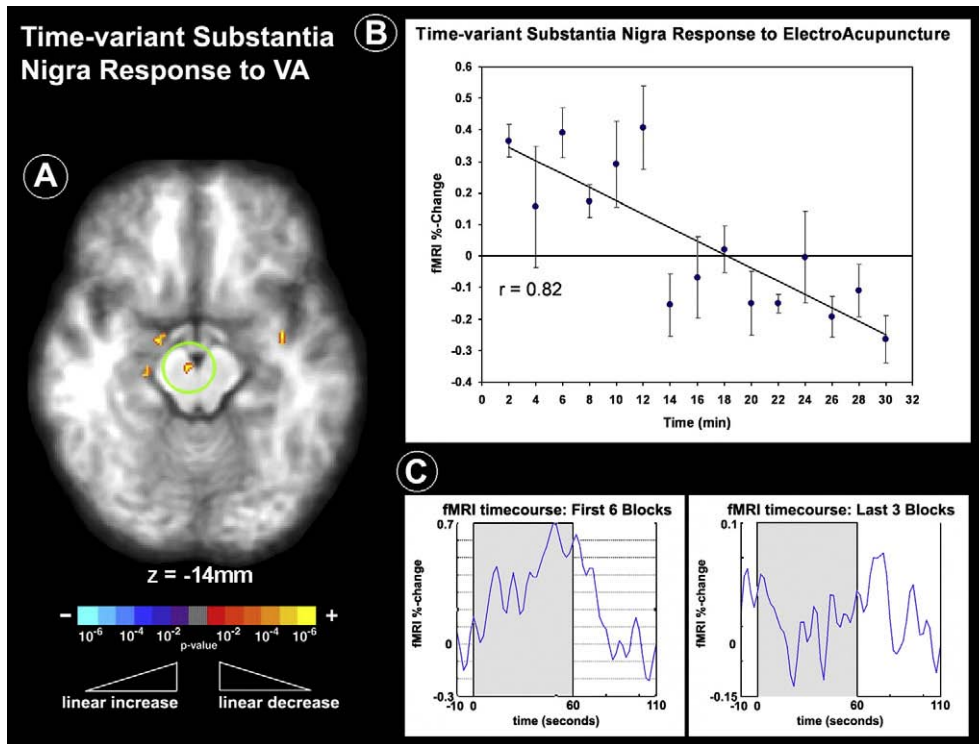


Fig. 5. Verum acupuncture (VA) response in the substantia nigra (A) demonstrated linearly decreasing bimodal response over time – initial activation and later deactivation (B). (C) There was a fundamentally different fMRI response to VA in this brain region during the first 6 blocks (activation), compared to the last 3 blocks (deactivation).

with arousal and the hypothalamic–pituitary–axis stress response, relaying afferent signaling to the hypothalamus and amygdala (Ziegler et al., 1999). Thus, deactivation in the human LC is consistent with decreased stress response during VA.

The PAG is an important region for endogenous opioidergic neurotransmission and has been noted in past animal studies, which report acupuncture activation of opioid neurotransmission (Guo et al., 2004). Our results showed that VA induced deactivation in the caudal PAG, and activation in the rostral ventrolateral PAG, which was greater for VA compared to SPA. Animal studies have demonstrated that deep, inescapable muscle pain (similar to acupuncture) can induce an opioid-mediated cardio-depressor “quiescence” response governed by

the ventrolateral PAG, and distinct from a cardiopressor response mediated by the lateral and dorsolateral PAG (Bandler and Shipley, 1994; Keay et al., 2001; Lumb, 2002). Clearly, our results demonstrate that acupuncture modulates the PAG and, possibly, opioidergic systems, though the implications of different rostro-caudal response needs further work. For instance, this response may relate to acupuncture analgesia and could be associated with the deactivation seen in the NCF, a region known to be interconnected with the PAG and activated by electrical visceral (Dunckley et al., 2005) and heat (Moulton et al., 2008) pain stimuli in previous fMRI studies. Future work should attempt to link this modulation with activation and/or deactivation of opioid neurotransmission, as well as determine the

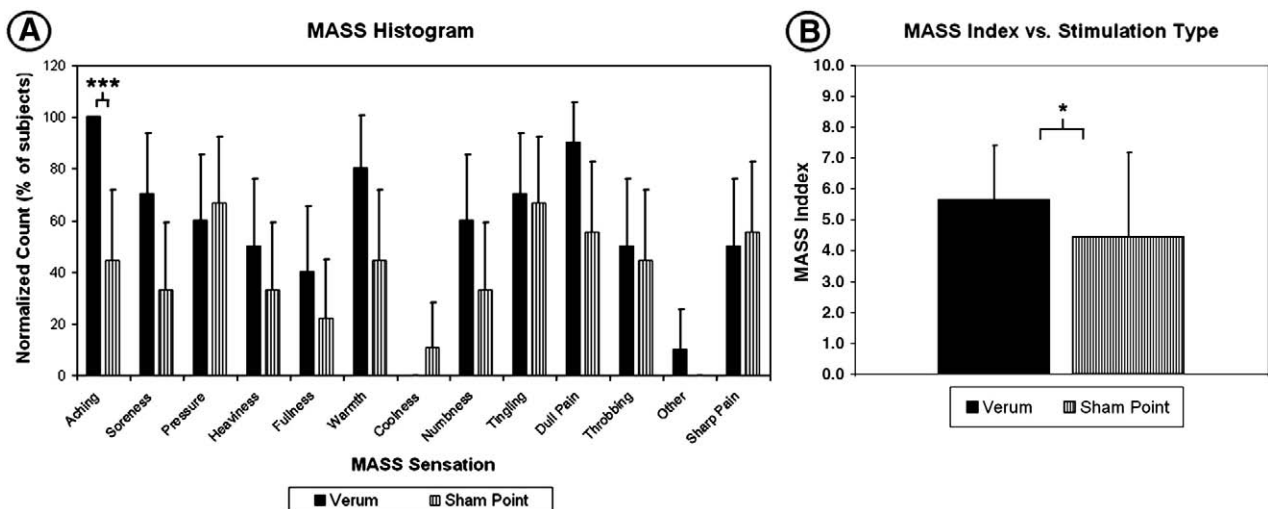
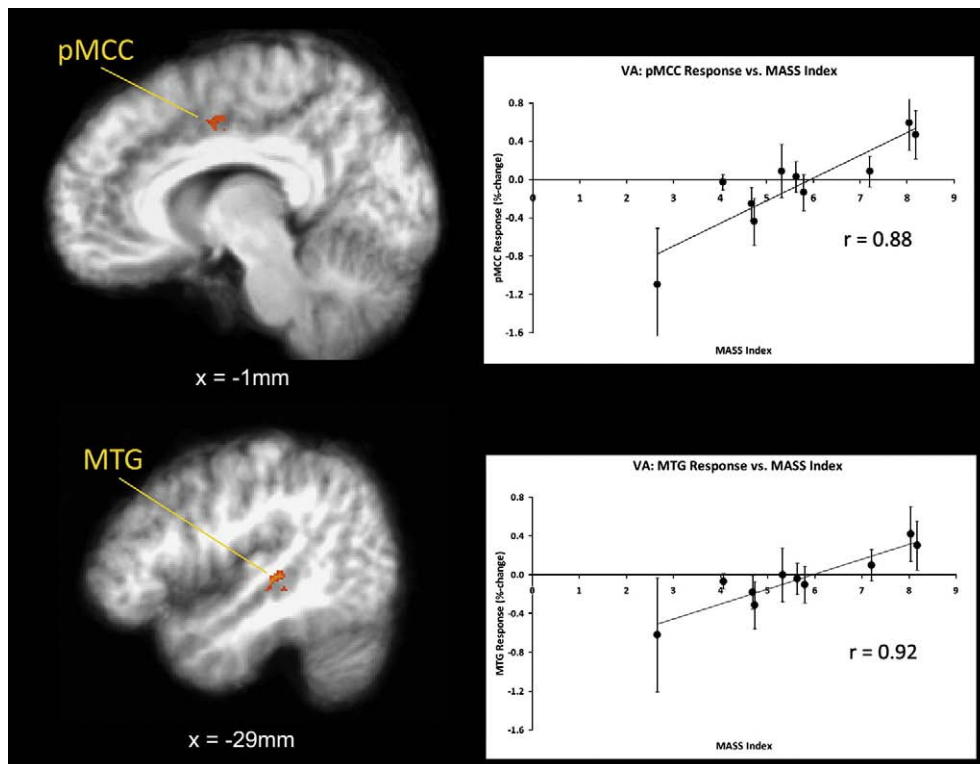


Fig. 6. Psychophysical Analysis using the MASS scale. (A) A histogram reflecting the prevalence of different sensations illustrates that verum (VA) and sham point (SPA) acupuncture elicited different types of sensations. VA more frequently induced “aching,” compared to SPA. (B) The MASS-index, a measure of sensation intensity, was greater for VA compared to SPA. n.b. Error bars in (A) represent a 90% confidence interval for binomial distribution. Sensations on the abscissa are in the order presented to the subjects. Error bars in B represent standard deviation. \* $p < 0.05$ , \*\*\* $p < 0.005$ .



**Fig. 7.** Covariation of sensation intensity with brain response. Subjects with greater sensation intensity (as measured by the MASS-index) had greater brain response to VA stimulation in (A) the posterior Middle Cingulate Cortex (pMCC), and (B) middle temporal gyrus (MTG). No significant covariation was found for SPA.

autonomic correlates to acupuncture-induced brainstem response in the human.

#### Differences in brain response: VA versus SPA

In general, both main effects and time-variant response was more robust in limbic and brainstem regions for VA compared to SPA. It is noteworthy that VA also induced more varied and stronger sensations, even with similar current intensity, and that sensation intensity covaried with specific brain response for VA. These results suggest that stimulus location in acupuncture may be an important factor in modulating brain activity in limbic structures, but may be due to the differences in psychophysical response.

In general, the “active ingredient” of acupuncture is not known; a fact which motivates research into acupuncture mechanism (Hammerschlag and Zwickey, 2006). Based on our cumulative results, we hypothesize that stimulation of peripheral nerve receptors in deep muscular and/or fascial tissue (which varies between different body locations) is fundamental to eliciting significant *deqi* sensation. This afference is transferred to the central nervous system, initiating a cascade of events at the level of the brain, which can be studied by neuroimaging. Furthermore, while needle insertion can be accomplished anywhere in the body, we suggest that certain points on the body are more efficient (e.g. receptor density) to maximize afference and so-called “*deqi*” sensation. These efficient points may or may not be traditional acupoints, as highly significant brain modulation in limbic structures has been noted by previous studies using sham point stimulation (Kong et al., 2007b; Wu et al., 2002). This “point efficiency” hypothesis might explain why, for knee osteoarthritis, insertive needling at non-acupoints may produce clinically significant improvement relative to conventional therapy (Scharf et al., 2006), while verum acupuncture at efficient locations (acupoints) on the body might maximize clinical response (Berman et al., 2004). However, this assumes that (as suggested in many acupuncture texts (Cheng, 1996)) clinical response is linked to acupuncture

sensation — a correlation that awaits more scientific testing. Thus, whether our hypothesis extends to other chronic pain conditions (e.g. fibromyalgia) or even to non-pain pathology (e.g. insomnia, anxiety) remains to be seen.

#### Technical considerations and limitations

Several limitations in our study design should be discussed. Firstly, as we used cardiac-gated fMRI, our field of view could not cover the entire brain. As our hypotheses were focused primarily on brainstem regions, we chose to exclude the most anterior and posterior portions of the forebrain (including SI, ACC and anterior insula). We preferred to compromise brain coverage for improved fidelity in the brain regions we did image. Secondly, our time-variant analysis used a linear ramp contrast. Other non-linear response patterns may indeed have occurred, and, in fact, the VA response in several limbic regions such as the amygdala and SN appears to be better fit by non-linear patterns. However, it is important to note that a linear contrast was still sensitive to non-linear time-variant response in these regions, in addition to being sensitive to more straightforward habituation in somatosensory areas. Moreover, a linear contrast has the advantage of easy interpretability and can be considered adequate for a first cut attempt to resolve time-variant brain response.

#### Conclusions

In conclusion, our results provide human neuroimaging evidence that acupuncture modulates activity in brainstem nuclei important to endogenous monoaminergic and opioidergic systems. Activation in the ventrolateral PAG was greater for VA compared to SPA. Furthermore, linearly decreasing fMRI activation was observed for both VA and SPA in sensorimotor brain regions (SII, posterior insula, PMC), which we attributed to habituation. Additionally, VA produced linearly time-variant fMRI response in limbic regions, such as the amygdala, hippocampus, and SN. This response was not likely to be habituation,

as it was bimodal, consisting of early activation and transitioning to delayed deactivation by the end of the scan run. Future studies should explore the clinical significance of this interesting time-variant pattern of brain response. These data show that acupuncture induces different brain response early in the course of stimulation, compared to 20–30 min after stimulation has commenced. We attribute differences in fMRI response between VA and SPA to the more varied and stronger psychophysical response induced by VA. Our study demonstrates that acupuncture-induced brainstem response can be studied non-invasively in humans, allowing for comparison to animal studies. Our protocol also demonstrates a fMRI approach to study habituation and other time-variant phenomena (e.g. memory consolidation, etc.) over longer durations of time.

### Acknowledgments

We would like to thank the National Center for Complementary and Alternative Medicine, NIH for funding support: K01-AT002166 (to VN), P01-AT002048 (VN, KKSH), K01-AT004481 (RD), F05-AT003770 (KP) and K24-AT004095. We also acknowledge the National Institute of Neurological Disorders and Stroke (K25-NS057580 to PLP), the NCCR (P41-RR14075, GCRC M01-RR01066), and the Mental Illness and Neuroscience Discovery (MIND) Institute. Dr. Park was also supported by the Institute of Information Technology Advancement, Korea IITA-2008-(C1090-0801-0002). Dr. Harris was also supported by Department of Army grant DAMD-Award Number W81XWH-07-2-0050, and Dana Foundation Award in Brain and Immuno-imaging. The content is solely the responsibility of the authors and does not necessarily represent the official views of our funding agencies.

### Appendix A. Supplementary data

Supplementary data associated with this article can be found, in the online version, at doi:10.1016/j.neuroimage.2009.03.060.

### References

- Bandler, R., Shipley, M.T., 1994. Columnar organization in the midbrain periaqueductal gray: modules for emotional expression? *Trends Neurosci.* 17, 379–389.
- Becerra, L.R., Breiter, H.C., Stojanovic, M., Fishman, S., Edwards, A., Comite, A.R., Gonzalez, R.G., Borsook, D., 1999. Human brain activation under controlled thermal stimulation and habituation to noxious heat: an fMRI study. *Magn. Reson. Med.* 41, 1044–1057.
- Becerra, L., Breiter, H.C., Wise, R., Gonzalez, R.G., Borsook, D., 2001. Reward circuitry activation by noxious thermal stimuli. *Neuron* 32, 927–946.
- Beckmann, C.F., Smith, S.M., 2004. Probabilistic independent component analysis for functional magnetic resonance imaging. *IEEE Trans. Med. Imaging* 23, 137–152.
- Berman, B.M., Lao, L., Langenberg, P., Lee, W.L., Gilpin, A.M., Hochberg, M.C., 2004. Effectiveness of acupuncture as adjunctive therapy in osteoarthritis of the knee: a randomized, controlled trial. *Ann. Intern. Med.* 141, 901–910.
- Bloom, F., Guillemin, R., 1978. Neurons containing b-endorphin in rat brain exist separately from those containing enkephalin: immunocytochemical studies. *Proc. Natl. Acad. Sci. U. S. A.* 75, 1591–1595.
- Buckner, R.L., Andrews-Hanna, J.R., Schacter, D.L., 2008. The brain's default network: anatomy, function, and relevance to disease. *Ann. N.Y. Acad. Sci.* 1124, 1–38.
- Cheng, X., 1996. *Chinese Acupuncture and Moxibustion*. Beijing Foreign Languages Press, Beijing.
- Cheng, R.S., Pomeranz, B., 1981. Monoaminergic mechanism of electroacupuncture analgesia. *Brain Res.* 215, 77–92.
- Corfield, D.R., Murphy, K., Josephs, O., Fink, G.R., Frackowiak, R.S., Guz, A., Adams, L., Turner, R., 1999. Cortical and subcortical control of tongue movement in humans: a functional neuroimaging study using fMRI. *J. Appl. Physiol.* 86, 1468–1477.
- Cox, R.W., 1996. AFNI: software for analysis and visualization of functional magnetic resonance neuroimages. *Comput. Biomed. Res.* 29, 162–173.
- Craig, A.D., Chen, K., Bandy, D., Reiman, E.M., 2000. Thermosensory activation of insular cortex. *Nat. Neurosci.* 3, 184–190.
- Dagli, M.S., Ingeholm, J.E., Haxby, J.V., 1999. Localization of cardiac-induced signal change in fMRI. *Neuroimage* 9, 407–415.
- DaSilva, A.F., Becerra, L., Makris, N., Strassman, A.M., Gonzalez, R.G., Geatrakis, N., Borsook, D., 2002. Somatotopic activation in the human trigeminal pain pathway. *J. Neurosci.* 22, 8183–8192.
- Derbyshire, S.W., Jones, A.K., Gyulai, F., Clark, S., Townsend, D., Firestone, L.L., 1997. Pain processing during three levels of noxious stimulation produces differential patterns of central activity. *Pain* 73, 431–445.
- Dhond, R.P., Kettner, N., Napadow, V., 2007. Neuroimaging acupuncture effects in the human brain. *J. Altern. Complement. Med.* 13, 603–616.
- Dhond, R.P., Yeh, C., Park, K., Kettner, N., Napadow, V., 2008. Acupuncture modulates resting state connectivity in default and sensorimotor brain networks. *Pain* 136, 407–418.
- Dunkley, P., Wise, R.G., Fairhurst, M., Hobden, P., Aziz, Q., Chang, L., Tracey, I., 2005. A comparison of visceral and somatic pain processing in the human brainstem using functional magnetic resonance imaging. *J. Neurosci.* 25, 7333–7341.
- Glover, G.H., Li, T.Q., Ress, D., 2000. Image-based method for retrospective correction of physiological motion effects in fMRI: RETROICOR. *Magn. Reson. Med.* 44, 162–167.
- Griswold, M.A., Jakob, P.M., Heidemann, R.M., Nittka, M., Jellus, V., Wang, J., Kiefer, B., Haase, A., 2002. Generalized autocalibrating partially parallel acquisitions (GRAPPA). *Magn. Reson. Med.* 47, 1202–1210.
- Guimaraes, A.R., Melcher, J.R., Talavage, T.M., Baker, J.R., Ledden, P., Rosen, B.R., Kiang, N.Y., Fullerton, B.C., Weisskoff, R.M., 1998. Imaging subcortical auditory activity in humans. *Hum. Brain Mapp.* 6, 33–41.
- Guo, Z.L., Moazzami, A.R., Longhurst, J.C., 2004. Electroacupuncture induces c-Fos expression in the rostral ventrolateral medulla and periaqueductal gray in cats: relation to opioid containing neurons. *Brain Res.* 1030, 103–115.
- Hackett, T.A., Smiley, J.F., Ulbert, I., Karmos, G., Lakatos, P., de la Mothe, L.A., Schroeder, C.E., 2007. Sources of somatosensory input to the caudal belt areas of auditory cortex. *Perception* 36, 1419–1430.
- Hammerschlag, R., Zwickey, H., 2006. Evidence-based complementary and alternative medicine: back to basics. *J. Altern. Complement. Med.* 12, 349–350.
- Han, J., 1998. *The Neurochemical Basis of Pain Relief by Acupuncture*. Hubei Science and Technology Press, Hubei.
- Han, J.S., 2004. Acupuncture and endorphins. *Neurosci. Lett.* 361, 258–261.
- Han, C.S., Chou, P.H., Lu, C.C., Lu, L.H., Yang, T.H., Jen, M.F., 1979. The role of central 5-hydroxytryptamine in acupuncture analgesia. *Sci. Sin.* 22, 91–104.
- Han, S.H., Yoon, S.H., Cho, Y.W., Kim, C.J., Min, B.I., 1999. Inhibitory effects of electroacupuncture on stress responses evoked by tooth-pulp stimulation in rats. *Physiol. Behav.* 66, 217–222.
- Hsieh, J.C., Stone-Elander, S., Ingvar, M., 1999. Anticipatory coping of pain expressed in the human anterior cingulate cortex: a positron emission tomography study. *Neurosci. Lett.* 262, 61–64.
- Hui, K.K., Liu, J., Makris, N., Gollub, R.L., Chen, A.J., Moore, C.I., Kennedy, D.N., Rosen, B.R., Kwong, K.K., 2000. Acupuncture modulates the limbic system and subcortical gray structures of the human brain: evidence from fMRI studies in normal subjects. *Hum. Brain Mapp.* 9, 13–25.
- Hui, K.K., Liu, J., Marina, O., Napadow, V., Haselgrove, C., Kwong, K.K., Kennedy, D.N., Makris, N., 2005. The integrated response of the human cerebro-cerebellar and limbic systems to acupuncture stimulation at ST 36 as evidenced by fMRI. *Neuroimage* 27, 479–496.
- Hui, K.K., Nixon, E.E., Vangel, M.G., Liu, J., Marina, O., Napadow, V., Hodge, S.M., Rosen, B.R., Makris, N., Kennedy, D.N., 2007. Characterization of the “Deqi” response in acupuncture. *BMC Complement. Altern. Med.* 7, 33.
- Keay, K.A., Clement, C.L., Depaulis, A., Bandler, R., 2001. Different representations of inescapable noxious stimuli in the periaqueductal gray and upper cervical spinal cord of freely moving rats. *Neurosci. Lett.* 313, 17–20.
- Kong, J., Gollub, R., Huang, T., Polich, G., Napadow, V., Hui, K., Vangel, M., Rosen, B., Kaptchuk, T.J., 2007a. Acupuncture de qi, from qualitative history to quantitative measurement. *J. Altern. Complement. Med.* 13, 1059–1070.
- Kong, J., Gollub, R.L., Webb, J.M., Kong, J.T., Vangel, M.G., Kwong, K., 2007b. Test-retest study of fMRI signal change evoked by electroacupuncture stimulation. *Neuroimage* 34, 1171–1181.
- Kwon, Y., Kang, M., Ahn, C., Han, H., Ahn, B., Lee, J., 2000. Effect of high or low frequency electroacupuncture on the cellular activity of catecholaminergic neurons in the brain stem. *Acupunct. Electrother. Res.* 25, 27–36.
- Li, A., Wang, Y., Xin, J., Lao, L., Ren, K., Berman, B.M., Zhang, R.X., 2007. Electroacupuncture suppresses hyperalgesia and spinal Fos expression by activating the descending inhibitory system. *Brain Res.* 1186, 171–179.
- Liu, W.C., Feldman, S.C., Cook, D.B., Hung, D.L., Xu, T., Kalnin, A.J., Komisaruk, B.R., 2004. fMRI study of acupuncture-induced periaqueductal gray activity in humans. *Neuroreport* 15, 1937–1940.
- Lumb, B.M., 2002. Inescapable and escapable pain is represented in distinct hypothalamic-midbrain circuits: specific roles for Delta- and C-nociceptors. *Exp. Physiol.* 87, 281–286.
- Mai, J., Assheuer, J., Paxinos, G., 2004. *Atlas of the Human Brain*. Elsevier Academic Press, San Diego.
- Mainiero, C., Zhang, W.T., Kumar, A., Rosen, B.R., Sorensen, A.G., 2007. Mapping the spinal and supraspinal pathways of dynamic mechanical allodynia in the human trigeminal system using cardiac-gated fMRI. *Neuroimage* 35, 1201–1210.
- Malinen, S., Schurmann, M., Hlushchuk, Y., Forss, N., Hari, R., 2006. Improved differentiation of tactile activations in human secondary somatosensory cortex and thalamus using cardiac-triggered fMRI. *Exp. Brain Res.* 174, 297–303.
- Mann, F., 1974. Acupuncture analgesia. Report of 100 experiments. *Br. J. Anaesth.* 46, 361–364.
- Mayer, D.J., 2000. Biological mechanisms of acupuncture. *Prog. Brain Res.* 122, 457–477.
- Meredith, M.A., Stein, B.E., 1986. Visual, auditory, and somatosensory convergence on cells in superior colliculus results in multisensory integration. *J. Neurophysiol.* 56, 640–662.
- Moulton, E.A., Burstein, R., Tully, S., Hargreaves, R., Becerra, L., Borsook, D., 2008. Interictal dysfunction of a brainstem descending modulatory center in migraine patients. *PLoS ONE* 3, e3799.
- Nagy, A., Kruse, W., Rottmann, S., Dannenberg, S., Hoffmann, K.P., 2006. Somatosensory-motor neuronal activity in the superior colliculus of the primate. *Neuron* 52, 525–534.

- Napadow, V., Dhond, R.P., Purdon, P., Kettner, N., Makris, N., Kwong, K.K., Hui, K.K., 2005a. Correlating acupuncture fMRI in the human brainstem with heart rate variability. *Conf. Proc. IEEE Eng. Med. Biol. Soc.* 5, 4496–4499.
- Napadow, V., Makris, N., Liu, J., Kettner, N.W., Kwong, K.K., Hui, K.K., 2005b. Effects of electroacupuncture versus manual acupuncture on the human brain as measured by fMRI. *Hum. Brain Mapp.* 24, 193–205.
- Napadow, V., Dhond, R., Kennedy, D., Hui, K.K., Makris, N., 2006. Automated brainstem co-registration (ABC) for MRI. *Neuroimage* 32, 1113–1119.
- Napadow, V., Kettner, N., Liu, J., Li, M., Kwong, K.K., Vangel, M., Makris, N., Audette, J., Hui, K.K., 2007. Hypothalamus and amygdala response to acupuncture stimuli in Carpal Tunnel Syndrome. *Pain* 130, 254–266.
- Napadow, V., Dhond, R., Conti, G., Makris, N., Brown, E.N., Barbieri, R., 2008. Brain correlates of autonomic modulation: combining heart rate variability with fMRI. *Neuroimage*.
- Oldfield, R.C., 1971. The assessment and analysis of handedness: the Edinburgh inventory. *Neuropsychologia* 9, 97–113.
- Parent, A., 1996. *Carpenter's Human Neuroanatomy*, 9th ed. Williams & Wilkins, Baltimore.
- Paxinos, G., Huang, X.-F., 1995. *Atlas of the Human Brainstem*. Academic Press, San Diego.
- Petrides, M., 2005. Lateral prefrontal cortex: architectonic and functional organization. *Philos. Trans. R. Soc. Lond., B Biol. Sci.* 360, 781–795.
- Petrovic, P., Ingvar, M., 2002. Imaging cognitive modulation of pain processing. *Pain* 95, 1–5.
- Petrovic, P., Ingvar, M., Stone-Elander, S., Petersson, K.M., Hansson, P., 1999. A PET activation study of dynamic mechanical allodynia in patients with mononeuropathy. *Pain* 83, 459–470.
- Petrovic, P., Carlsson, K., Petersson, K.M., Hansson, P., Ingvar, M., 2004. Context-dependent deactivation of the amygdala during pain. *J. Cogn. Neurosci.* 16, 1289–1301.
- Pomeranz, B., 2001. Acupuncture analgesia – basic research. In: Stux, G., Hammerschlag, R. (Eds.), *Clinical Acupuncture: Scientific Basis*. Springer, Berlin, pp. 1–28.
- Pomeranz, B., Chiu, D., 1976. Naloxone blockade of acupuncture analgesia: endorphin implicated. *Life Sci.* 19, 1757–1762.
- Poncelet, B.P., Wedeen, V.J., Weisskoff, R.M., Cohen, M.S., 1992. Brain parenchyma motion: measurement with cine echo-planar MR imaging. *Radiology* 185, 645–651.
- Raichle, M.E., MacLeod, A.M., Snyder, A.Z., Powers, W.J., Gusnard, D.A., Shulman, G.L., 2001. A default mode of brain function. *Proc. Natl. Acad. Sci. U. S. A.* 98, 676–682.
- Sah, P., Faber, E.S., Lopez De Armentia, M., Power, J., 2003. The amygdaloid complex: anatomy and physiology. *Physiol. Rev.* 83, 803–834.
- Scharf, H.P., Mansmann, U., Streitberger, K., Witte, S., Kramer, J., Maier, C., Trampisch, H.J., Victor, N., 2006. Acupuncture and knee osteoarthritis: a three-armed randomized trial. *Ann. Intern. Med.* 145, 12–20.
- Thompson, R.F., Spencer, W.A., 1966. Habituation: a model phenomenon for the study of neuronal substrates of behavior. *Psychol. Rev.* 73, 16–43.
- Tjen-A-Looi, S.C., Li, P., Longhurst, J.C., 2004. Medullary substrate and differential cardiovascular responses during stimulation of specific acupoints. *Am. J. Physiol. Regul. Integr. Comp. Physiol.* 287, R852–862.
- Vincent, C.A., Richardson, P.H., Black, J.J., Pither, C.E., 1989. The significance of needle placement site in acupuncture. *J. Psychosom. Res.* 33, 489–496.
- Vogt, B.A., 2005. Pain and emotion interactions in subregions of the cingulate gyrus. *Nat. Rev., Neurosci.* 6, 533–544.
- Wang, Y.Q., Cao, X.D., Wu, G.C., 1999. Role of dopamine receptors and the changes of the tyrosine hydroxylase mRNA in acupuncture analgesia in rats. *Acupunct. Electrother. Res.* 24, 81–88.
- Wu, M.T., Sheen, J.M., Chuang, K.H., Yang, P., Chin, S.L., Tsai, C.Y., Chen, C.J., Liao, J.R., Lai, P.H., Chu, K.A., Pan, H.B., Yang, C.F., 2002. Neuronal specificity of acupuncture response: a fMRI study with electroacupuncture. *Neuroimage* 16, 1028–1037.
- Zald, D.H., 2003. The human amygdala and the emotional evaluation of sensory stimuli. *Brain Res. Brain Res. Rev.* 41, 88–123.
- Zhang, W.T., Mainiero, C., Kumar, A., Wiggins, C.J., Benner, T., Purdon, P.L., Bolar, D.S., Kwong, K.K., Sorensen, A.G., 2006. Strategies for improving the detection of fMRI activation in trigeminal pathways with cardiac gating. *Neuroimage* 31, 1506–1512.
- Zhou, W.Y., Tjen-A-Looi, S.C., Longhurst, J.C., 2005. Brain stem mechanisms underlying acupuncture modality-related modulation of cardiovascular responses in rats. *J. Appl. Physiol.* 99, 851–860.
- Ziegler, D.R., Cass, W.A., Herman, J.P., 1999. Excitatory influence of the locus coeruleus in hypothalamic–pituitary–adrenocortical axis responses to stress. *J. Neuroendocrinol.* 11, 361–369.